


# San-Zhong-Kui-Jian-Tang Exerts Antitumor Effects Associated With Decreased Cell Proliferation and Metastasis by Targeting ERK and the Epithelial–Mesenchymal Transition Pathway in Oral Cavity Squamous Cell Carcinoma

Integrative Cancer Therapies  
Volume 21: 1–18  
© The Author(s) 2022  
Article reuse guidelines:  
sagepub.com/journals-permissions  
DOI: 10.1177/15347354221134921  
journals.sagepub.com/home/ict  


Pei-Yu Hsu, MD<sup>1,2</sup>, Jiun-Liang Chen, PhD<sup>1,3</sup>, Shun-Li Kuo, MD<sup>1,2,3</sup>,  
Wan-Ling Wang, BS<sup>4,5</sup>, Fei-Wen Jan, MS<sup>5</sup>, Sien-Hung Yang, PhD<sup>1,2,3,6</sup>,  
and Chia-Yu Yang<sup>4,5,7,8</sup>

## Abstract

**Background:** Oral squamous cell carcinoma (OSCC) is an aggressive cancer whose 5-year survival rate remains poor. San-Zhong-Kui-Jian-Tang (SZKJT), a Chinese herbal formula, has long been used in clinical practice as adjuvant therapy in cancers. However, its therapeutic effects and molecular mechanisms in OSCC remain unclear. **Methods:** We investigated the potential therapeutic effects and molecular mechanism of SZKJT in OSCC in tumor cell lines and in tumor xenograft mice and evaluated combined SZKJT and cisplatin treatment efficacy. In vitro-cultured OSCC cells were administered SZKJT at different doses or SZKJT plus cisplatin, and cell proliferation, colony formation assays, and cell cycle analysis were used to assess the effects on cancer cell proliferation and apoptosis. We also analyzed the effects of SZKJT on oral cancer cell line migration, the regulation of mitogen-activated protein kinase (MAPK) signaling, and epithelial-mesenchymal transition (EMT)-associated genes. The antitumor effects of SZKJT plus cisplatin were also tested in vivo using a tumor-bearing NOD/SCID mice model. **Results:** The results showed that SZKJT effectively inhibited OSCC cell proliferation, induced cell cycle S phase arrest, and induced cell apoptosis. SZKJT also inhibited cell migration by modulating the MAPK signaling and epithelial-mesenchymal transition (EMT) pathway. Further exploration suggested that SZKJT affects OSCC by modulating ERK pathway; downregulating vimentin, fibronectin, and Oct-4; and upregulating E-cadherin. In vivo, SZKJT significantly inhibited tumor growth, and SZKJT and cisplatin exerted synergistic antitumor effects in model animals. **Conclusions:** SZKJT exerts antitumor effects in OSCC cells. Additionally, SZKJT and cisplatin exhibit synergy in OSCC treatment. These findings support the clinical usage of Chinese herbal formulas as adjuvant therapy with chemotherapy in cancer treatment.

## Keywords

San-Zhong-Kui-Jian-Tang, oral cavity squamous cell carcinoma, cancer therapy, Chinese medicine

Submitted March 25, 2022; revised September 22, 2022; accepted October 11, 2022

## Introduction

Oral squamous cell carcinoma (OSCC) is one of the most common cancers worldwide,<sup>1,2</sup> and its global incidence is increasing, especially in Asia.<sup>3</sup> In Taiwan, oral, oropharyngeal, and hypopharyngeal cancers ranked fourth among all cancers in men in terms of both incidence and mortality rate. Furthermore, oral, oropharyngeal, and hypopharyngeal cancers ranked fifth in terms of cancer deaths according to the Taiwan Cancer Registry Annual Report in 2017.

OSCC is also associated with high morbidity.<sup>4</sup> Despite advances in treatment modalities such as surgery, radiation, and chemotherapy in recent years, the prognosis of OSCC patients remains poor.<sup>5</sup> Some patients may suffer from severe side effects during conventional cancer treatments, which may delay or interrupt treatment. Therefore, new and effective therapeutic agents that are safe and exhibit minimal toxicity could improve the quality of life of OSCC patients and are urgently needed.



Systematic reviews have shown that traditional Chinese medicines (TCMs), such as Astragalus, ginseng, and turmeric, can enhance the efficacy of chemotherapy and radiotherapy (RT) and reduce side effects after therapy via antioxidant, anti-inflammatory, immunomodulatory, and anticancer mechanisms.<sup>6,7</sup> TCMs have also been shown to have a hepatoprotective effect during chemotherapy.<sup>8</sup> One study investigated patients with nasopharyngeal carcinoma who received conventional cancer treatments combined with TCM and found reduced rates of adverse effects, improved performance, augmented immunostimulation, an enhanced tumor response, and increased survival rates compared to those without TCM.<sup>9</sup> Previous study showed that head and neck cancer patients who received conventional cancer treatments combined with TCM (to clear heat, supplement yin, and boost qi) experienced less weight loss during RT than those who only received conventional cancer treatments (the mean weight change was  $-5.43\%$  in the study group and  $-7.63\%$  in the control group,  $P=.016$ ), and this effect was enhanced when patients received TCM for a longer duration ( $-3.77\%$  vs  $-7.63\%$ ,  $P=.001$ ). Compared to the control group, the study group also had significantly lower scores for “lack of appetite” on the M.D. Anderson Symptom Inventory ( $P=.002$ ).<sup>10</sup> In addition, in another study, we demonstrated that treatment with the TCM Gan Lu Yin during RT for head and neck cancer reduced the severity of xerostomia, and no impairment of hepatic or renal function was detected after TCM treatment.<sup>11</sup>

San-Zhong-Kui-Jian-Tang (SZKJT), a Chinese herbal formula, has been used to treat patients with various cancers in clinical practice for years. According to a report from Lin et al in 2015,<sup>12</sup> the use of adjunctive TCM therapy improved survival outcomes in head and neck cancer patients, and SZKJT is a common prescription (named San Zhong Hui Jian Shang in Lin’s article). SZKJT consists of 17 species of medicinal herbs. Previous studies have revealed that SZKJT exerts antitumor effects against breast cancer, colon cancer, hepatic cancer, and pancreatic carcinoma.<sup>13-18</sup> However, the

effects and molecular mechanisms of SZKJT against oral cancer remain unclear as they have not yet been reported.

In this study, we aimed to investigate the potential therapeutic effects and molecular mechanisms of SZKJT in OSCC both in vitro in tumor cell lines and in vivo in tumor xenograft mice and evaluate the efficacy of combined SZKJT and cisplatin treatment.

## Materials and Methods

### Preparation of SZKJT Extract

SZKJT consists of *Scutellaria baicalensis* Georgi, *Gentiana scabra* Bunge, *Trichosanthes kirilowii* Maxim., *Phellodendron chinense* C.K.Schneid., *Anemarrhena asphodeloides* Bunge, *Platycodon grandiflorus* (Jacq.) A.DC., *Laminaria japonica* Aresch., *Bupleurum chinense* DC., *Glycyrrhiza uralensis* Fisch., *Sparganium stoloniferum* (Graebn.) Buch.-Ham. ex Juz., *Curcuma phaeocaulis* Valetton, *Forsythia suspensa* (Thunb.) Vahl, *Pueraria lobata* (Willd.) Ohwi, *Paeonia lactiflora* Pall., *Angelica sinensis* (Oliv.) Diels, *Coptis chinensis* Franch., and *Cimicifuga dahurica* (Turcz.)Maxim.. The above herbal drugs were mixed with the ratio of 4.0 : 2.5 : 2.5 : 4.0 : 2.5 : 2.5 : 2.5 : 1.5 : 1.5 : 1.5 : 1.5 : 1.5 : 1.0 : 1.0 : 1.0 : 0.5 in order. The composition of SZKJT was shown in Supplemental Table S1. SZKJT extract was prepared following standard procedures according to the Taiwan Herbal Pharmacopeia (second edition). The herbal material was extracted by Chuang Song Zong Pharmaceutical Co., Ltd. under Good Manufacturing Practice (GMP) conditions. Each herb used to prepare the SZKJT extract was examined for heavy metals, pesticides, and microorganisms according to standard procedures established by the government of Taiwan. The crude drugs used to prepare SZKJT consisted of 17 herbal drugs weighing a total of 34 g. These herbs were decocted with boiling water, filtered, and extracted to 11.8 g. The final preparation was stored at  $-20^{\circ}\text{C}$  until use.

<sup>1</sup>Department of Traditional Chinese Medicine, Chang Gung Memorial Hospital, Taoyuan, Taiwan

<sup>2</sup>Graduate Institute of Clinical Medical Sciences, College of Medicine, Chang Gung University, Taoyuan, Taiwan

<sup>3</sup>School of Traditional Chinese Medicine, College of Medicine, Chang Gung University, Taoyuan, Taiwan

<sup>4</sup>Molecular Medicine Research Center, Chang Gung University, Taoyuan, Taiwan

<sup>5</sup>Department of Microbiology and Immunology, College of Medicine, Chang Gung University, Taoyuan, Taiwan

<sup>6</sup>Research Center for Chinese Herbal Medicine, Chang Gung University of Science and Technology, Taoyuan, Taiwan

<sup>7</sup>Department of Otolaryngology Head and Neck Surgery, Chang Gung Memorial Hospital, Taoyuan, Taiwan

<sup>8</sup>Graduate Institute of Biomedical Sciences, College of Medicine, Chang Gung University, Taoyuan, Taiwan

#### Corresponding Authors:

Chia-Yu Yang, Department of Microbiology and Immunology, College of Medicine, Chang Gung University, No. 259, Wenhua 1st Rd., Guishan Dist., Taoyuan City 33302, Taiwan.

Email: chiayu-yang@mail.cgu.edu.tw

Sien-Hung Yang, School of Traditional Chinese Medicine, College of Medicine, Chang Gung University, No. 259, Wenhua 1st Rd., Guishan Dist., Taoyuan City 33302, Taiwan.

Email: dryang@mail.cgu.edu.tw

The quality of the herbs was monitored by high-performance liquid chromatography (HPLC).

HPLC analysis was carried out on a Waters 2690 separation module (Waters Co., MA, USA) using a Waters 2996 photodiode array detector. Compounds were separated on a Cosmosil 5C18 AR II column (4.6'250mm, 5  $\mu$ m) and maintained at 30°C. The operating conditions were as follows: detection wavelength, 254nm; flow rate, 1.0mL/min; column temperature, 30°C; injection volume, 20  $\mu$ L. The gradient for elution consisted of eluents A and B (A: 0.03% H<sub>3</sub>PO<sub>4</sub> in H<sub>2</sub>O; B: MeOH) and followed the following profile: 0 to 110minutes, from A: 90% and B: 10% to A: 10% and B: 90%. Four batches of SZKJT were prepared and measured separately to identify phytochemical constituents. Baicalin (TFDA) at 98.58% purity, berberine chloride (USP) at 100% purity, puerarin (TFDA) at 99.38% purity, and gentiopicroside (NIFDC) at 96.90% purity were obtained as reference standards. We used a UV detection wavelength of 254nm to detect gentiopicroside, puerarin, berberine, and baicalin. The relative retention times compared to that of puerarin for gentiopicroside, puerarin, berberine, and baicalin were 0.809, 1, 1.470, and 2.189, respectively.

### Cell Culture

Cell lines (SAS, OC3, and OEC-M1 cells) were incubated in Roswell Park Memorial Institute (RPMI) 1640 medium (Thermo Fisher Scientific, USA) or Dulbecco's modified Eagle's medium (DMEM; Gibco, USA) containing 10% fetal bovine serum and penicillin-streptomycin (Gibco, USA). SAS cell line was derived from a poorly differentiated squamous cell carcinoma from human tongue primary lesion. OC3 cell line was established from an OSCC in a long-term betel chewer who did not smoke.<sup>19</sup> The OECM-1 human OSCC cell line was derived from surgical resection of a primary tumor of a Taiwanese male patient.<sup>20</sup> All cells were maintained as monolayers at 37°C in an atmosphere containing 5% CO<sub>2</sub>/air.

### 3-(4,5-Dimethylthiazol-2-yl)-2,5-diphenyltetrazolium bromide (MTT) Cell Proliferation Assay

The effect of SZKJT was tested in OSCC cell lines by MTT assay. Cells were treated with (1) no drugs (control), (2) SZKJT at different doses (31.25, 62.5, 125, 250, 500, or 1000  $\mu$ g/mL), (3) 2.5  $\mu$ M cisplatin, (4) 2.5  $\mu$ M cisplatin with SZKJT at different doses (31.25, 62.5, 125, 250, 500, or 1000  $\mu$ g/mL) (5) PD98059 (50  $\mu$ M), or (6) PD98059 (50  $\mu$ M) with SZKJT at different doses (31.25, 62.5, 125, 250, 500, or 1000  $\mu$ g/mL) for 48 hours in a 96-well cell culture plate. This was followed by the addition of MTT solution (5 mg/mL) into each well. After incubation for 1 hour at 37°C, DMSO was added to each well, and the absorbance at

540 nm was measured with a multiwall spectrophotometer (SpectraMax M2; Molecular Devices, USA).

### Cell Death Assay

Cells were treated with (1) no drugs (control) or (2) SZKJT at different doses (62.5, 125, 250, 500, 1000, or 2000  $\mu$ g/mL) for 48 hours in 6-cm dishes. Dead cells were counted as Annexin V and propidium iodide positive cells by a FITC Annexin V Apoptosis Detection Kit (Invitrogen, USA) using a flow cytometry (Attune NxT; Invitrogen, USA), and the data were analyzed with FlowJo software (Tree Star, Inc.).

### Cell Cycle Analysis

Cells were treated with no drugs or SZKJT at different doses for 24 hours in 6-cm dishes. The cells were harvested and washed with cold PBS. The cells were then fixed in 70% ethanol overnight, stained with 50  $\mu$ g/mL propidium iodide (Sigma-Aldrich, USA) on ice for 20 minutes and subjected to flow cytometry analysis. The DNA content of the cells was used to classify the cells into presynthetic growth phase (G0/G1), S-phase, and postsynthetic growth phase/mitosis (G2/M).

### Colony Formation Assay

A total of 300 to 800 cells were plated in 6-well cell culture plates and then treated with SZKJT at different concentrations. The cells were allowed to grow for 10 to 14 days, after which the colonies were fixed, stained with 0.5% crystal violet and counted.

### Wound Healing Assay

The ability of the cultured cells to migrate was evaluated by wound healing assay using ibidi culture inserts (ibidi GmbH, Germany). Cells were pretreated with SZKJT at different concentrations (55  $\mu$ g/mL SZKJT for SAS cells, 250  $\mu$ g/mL SZKJT for OC3 cells, and 405  $\mu$ g/mL SZKJT for OEC-M1 cells) for 24 hours, and the living cells were then seeded in 6-well culture plates with a 2-well culture insert at a density of  $3 \times 10^4$  cells per well for 16 hours of culture in medium without SZKJT treatment. A defined, cell-free gap was generated by removing the insert, and the cells were washed with PBS to remove nonadherent cells. The area of the cell-free gap was monitored at the indicated times (0, 4, and 6 hours) with a light microscope. We then quantified the areas in 3 fields per well using ImageJ for analysis. These experiments were performed independently 3 times.

### Transwell Migration Assay

Transwell migration assay was performed in a migration chamber with an 8- $\mu$ m pore size polycarbonate membrane

(Corning, Merck, USA). Cells were pretreated with different doses of SZKJT for 24 hours. And then, living cells were harvested and re-seeded in the upper chamber for migration in the medium without SZKJT treatment. After incubation for 24 hours, a cotton swab was used to remove non-migrated cells in the upper chamber and the filter from each treatment was individually stained with 2% crystal violet. Migrated cells adherent to the underside of the filter were stained and photographed and then counted under a light microscope ( $\times 200$ ).

### Immunoblot Assay

Cells were treated with the control or SZKJT at different doses for 24 hours in 10-cm dishes. The cells were then harvested, and the proteins were extracted. The cell lysates were separated on a 10% SDS-PAGE gel, after which the proteins were transferred onto a PVDF membrane and blocked with skim milk for 1 hour. Then, the membrane was incubated with a specific antibody against the targeted protein overnight at 4°C. An HRP-labeled specific secondary antibody was applied at room temperature for 1 hour. The expression levels of p-ERK, p-JNK, p-p38, cleaved PARP, vimentin, and fibronectin were analyzed by incubation with specific antibodies (Cell Signaling, USA) and then detected with an enhanced chemiluminescence detection kit (PerkinElmer, USA). The membrane was exposed to X-ray film. We then quantified the signals using ImageJ analytical software.

### Quantitative Reverse Transcription PCR

For quantitative reverse transcription PCR (qPCR), first-strand complementary DNA was synthesized from 1  $\mu$ g of total RNA using random hexamers (GeneDirex, Germany) and SuperScript III RT (Invitrogen, USA). The sequences of the primers were as follows: Vimentin-F (5'-AGATG GACAG GTTAT CAACG -3'), Vimentin-R (5'-GCACT TGAAA GCTGT TTCT-3'), Fibronectin-F (5'-GGCAA CTCTG TCAAC GAAG-3'), Fibronectin-R (5'-GCACT GGCAC AACAG TTTA-3'), E-cadherin-F (5'-TGACC ACCTT AGAGG TCAG-3'), E-cadherin-R (5'-GCAGC AGAAT CAGAA TTAGC-3'), Oct-4-F (5'-GAGAA GGATG TGGTC CGAG-3'), Oct-4-R (5'-ACTGG TCCCC CTGAG AAA-3'), TBP-F849 (5'-TGCTC ACCCC ACCAA CAATT TAG-3'), and TBP-R969 (5'-CTGGG TTTGA TCATT CTGTA GATTA A -3').

### In Vivo Drug Toxicity Test

Six- to 8-week-old C57BL/6 mice were purchased from the National Laboratory Animal Center in Taiwan. The animals were housed with food and water under the regulations of the Animal Care Committee of Chang Gung University. The protocol was approved by the Institutional Animal Care and Use Committee of Chang Gung University

(IACUC approval No. CGU107-194). The in vivo toxicity of SZKJT was tested using these mice. The mice were randomly assigned to control (250  $\mu$ L of PBS, oral) and SZKJT (5.2 g/kg SZKJT, oral) treatment groups (N=3-8 in each group). The drug or PBS was given 3 times a week for 3 weeks. The body weight of the mice was recorded twice per week. The levels of aspartate transaminase (AST), alanine aminotransferase (ALT), creatinine, albumin, and glucose were measured, and a complete blood count and differential count of white blood cells were obtained before (Day 0) and after (Day 21) treatment.

### Xenograft Model and In Vivo SZKJT and cisplatin treatment

Six- to 8-week-old male NOD/SCID mice were purchased from the National Laboratory Animal Center in Taiwan. The animals were housed with food and water under the regulations of the Animal Care Committee of Chang Gung University. The protocol was approved by the Institutional Animal Care and Use Committee of Chang Gung University (IACUC approval No. CGU107-194). The animals were maintained in a specific pathogen-free environment with a 12-hour light-dark cycle at 22°C to 24°C and 50% humidity. Meloxicam (1-2 mg/kg, subcutaneously, SC) would be given to the mouse for pain control. For mild pain, we would provide Meloxicam and the mouse would be re-evaluated every 24 hours. For moderate pain, the mouse would be re-evaluated every 8 to 12 hours after Meloxicam given, and if there was no improvement for 3 consecutive times, the mouse would be euthanized. If the mouse suffered from severe pain and could not be relieved 4 hours after Meloxicam given, the mouse would be euthanized. The mice in our experiments did not suffer from any mild to severe pain and therefore mice did not use Meloxicam. SAS cells ( $5 \times 10^5$ ) were subcutaneously injected into the right or left flank of NOD/SCID mice in a volume of 100  $\mu$ L. Tumor size and the body weights of the mice were measured throughout the experimental period with calipers, and tumor volume was calculated according to the following formula: tumor volume ( $\text{mm}^3$ ) =  $L \times W^2/2$ , where  $L$  is the length and  $W$  is the width. When the tumors reached an average volume of 200-300  $\text{mm}^3$ , the animals were assigned randomly to experimental and control groups. For the SZKJT experiments, the tumor-bearing mice were randomly assigned to 4 groups: the (1) vehicle control (300  $\mu$ L of sterile water/day, oral, 5 times per week), (2) cisplatin (5 mg/kg/day, intraperitoneal injection, 1 time per week), (3) SZKJT (5.2 g/kg/day, oral, 5 times per week), and (4) SZKJT (5.2 g/kg/day, oral, 5 times per week) combined with cisplatin (5 mg/kg/day, intraperitoneal injection, 1 time per week) groups. The treatments were given for 4 weeks. The tumor volume was measured with a caliper biweekly, and a tumor growth curve was calculated. After 28 days of treatment, the mice were sacrificed

under adequate anesthesia, and the tumor weights were recorded. The tumor growth curves of the vehicle control and different treatment groups were compared. The residual tumors were processed and imbedded in formalin for further pathological analysis. Hematoxylin & eosin (H&E) staining of paraffin-embedded mouse xenograft tumor sections was performed. Immunohistochemical (IHC) staining of a consecutive series of 4- $\mu$ m sections was performed. Tissue sections were subjected to antigen retrieval using Bond epitope retrieval solution 2 in a Bond-Max automated immunostainer (Leica Biosystems) and stained with antibodies against Ki67 and p-ERK. The remaining steps were performed in accordance with standard procedures.

### Statistical Analyses

The results of the *in vitro* and *in vivo* experiments are expressed as the mean  $\pm$  SEM. Between-group comparisons were performed with the nonparametric Mann-Whitney *U* test for 2 groups. A *P* value  $<.05$  was considered to indicate statistical significance, and all results were compared against the vehicle group.

## Results

### Phytochemical Analysis

The chromatogram of SZKJT obtained by HPLC is shown in Figure 1. Four major peaks corresponding to SZKJT were identified by HPLC fingerprinting. These peaks corresponded to gentiopicroside, puerarin, berberine, and baicalin, which were identified by comparison with the corresponding reference standards. The relative amounts (mg/g) of gentiopicroside, puerarin, berberine, and baicalin in SZKJT were  $3.16 \pm 0.03$ ,  $11.66 \pm 0.04$ ,  $2.79 \pm 0.01$ , and  $41.30 \pm 0.27$ , respectively.

### SZKJT Inhibited OSCC Cell Proliferation and Induced Cell Death

The potential antitumor effects of SZKJT *in vitro* were first tested in the SAS, OC3, and OEC-M1 cell lines by MTT and colony formation assays. The results showed that SZKJT inhibited proliferation in the OSCC cell lines in a dose-dependent manner (Figure 2A). The IC<sub>50</sub> values for SZKJT were 53.7  $\mu$ g/mL for SAS cells, 249.5  $\mu$ g/mL for OC3 cells, and 405.8  $\mu$ g/mL for OEC-M1 cells. In the colony formation assay, SZKJT also effectively inhibited colony formation in the SAS, OC3, and OEC-M1 cell lines (Figure 2B-D).

Given the significant inhibitory effect of SZKJT on OSCC cell proliferation, we next determined whether SZKJT could alter cell cycle progression. We measured the DNA content of SAS and OC3 cells treated with SZKJT at the indicated concentrations for 24 hours using PI staining

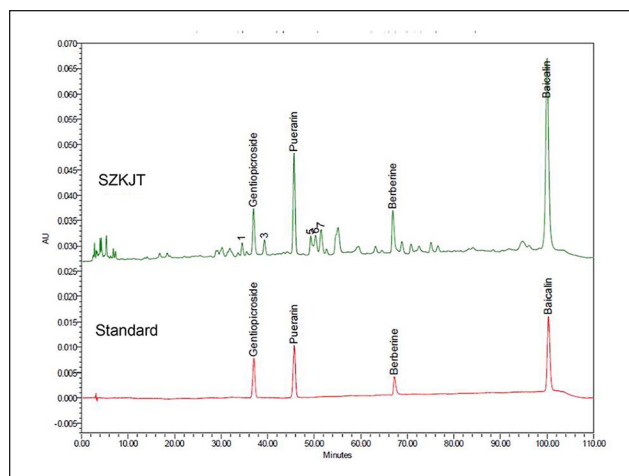


**Figure 1.** The chromatogram for SZKJT was obtained by HPLC analysis. HPLC chromatogram for SZKJT (upper panel) containing 4 major peaks that were identified by comparing retention times with those of the corresponding standards (lower panel).

and flow cytometry (Figure 3A). As shown in Figure 3B and C, SZKJT significantly increased the proportion of OSCC cells that were arrested in S phase, and the proportion of both SAS and OC3 cells in G<sub>2</sub>/M phase was decreased, especially in the high-dose treatment groups.

In addition, the effect of SZKJT on cell death in the OSCC cell lines was evaluated. SAS, OC3, and OEC-M1 cells were treated without (0  $\mu$ g/mL) or with SZKJT at different doses (62.5–2000  $\mu$ g/mL) for 48 hours. Compared with the control treatment, treatment with 500  $\mu$ g/mL SZKJT significantly increased the proportions of dead SAS cells by 42.23% (Figure 4A) and OC3 cells by 56.03% (Figure 4B) at 48 hours. Furthermore, SZKJT treatment significantly increased the proportion of dead OEC-M1 cells (Supplemental Figure S1). Treatment with SZKJT for 48 hours was found to have a dose-dependent effect on cell death in the 3 oral cancer cell lines. Poly(ADP-ribose) polymerase (PARP), a member of the PARP enzyme family, is an abundant DNA-binding enzyme that detects and signals DNA strand breaks.<sup>21</sup> The presence of cleaved PARP1 is one of the most commonly used diagnostic tools to detect cell death in many cell types.<sup>22</sup> In our experiment, the level of cleaved PARP was upregulated in SZKJT-treated SAS (Figure 4C). These results indicated that SZKJT not only suppresses OSCC cell growth but also inhibits cell proliferation and cell cycle progression. Additionally, SZKJT was found to induce cell death in OSCC.

### SZKJT Attenuated OSCC Cell Migration

The ability of OSCC cells to migrate was evaluated by wound healing assay and transwell migration assay after

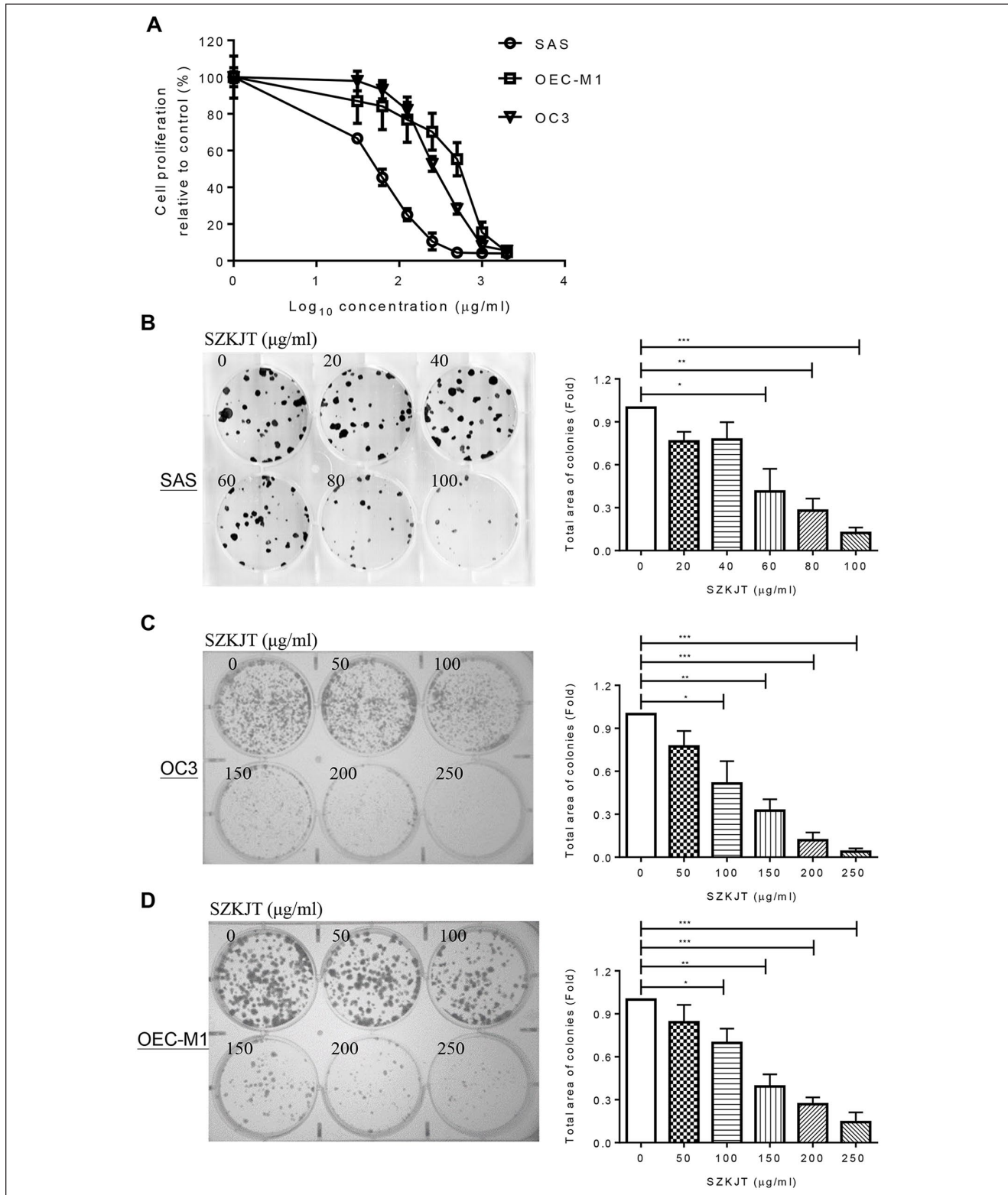


**Figure 2.** Inhibitory effects of SZKJT on the proliferation of OSCC cell lines. (A) Dose–response curves showing the cytotoxic effects of treatment with the SZKJT for 48 hours in SAS, OC3, and OEC-M1 cells, as assessed by MTT assays. The results are expressed as the percent cell proliferation relative to the proliferation of the control. Representative images and numbers of colonies formed by SAS (B), OC3 (C), and OEC-M1 (D) cells treated with SZKJT at different concentrations are shown. The results were obtained from 3 independent experiments. \*\*\* $P < .001$ ; \*\* $P < .01$ ; \* $P < .05$ .

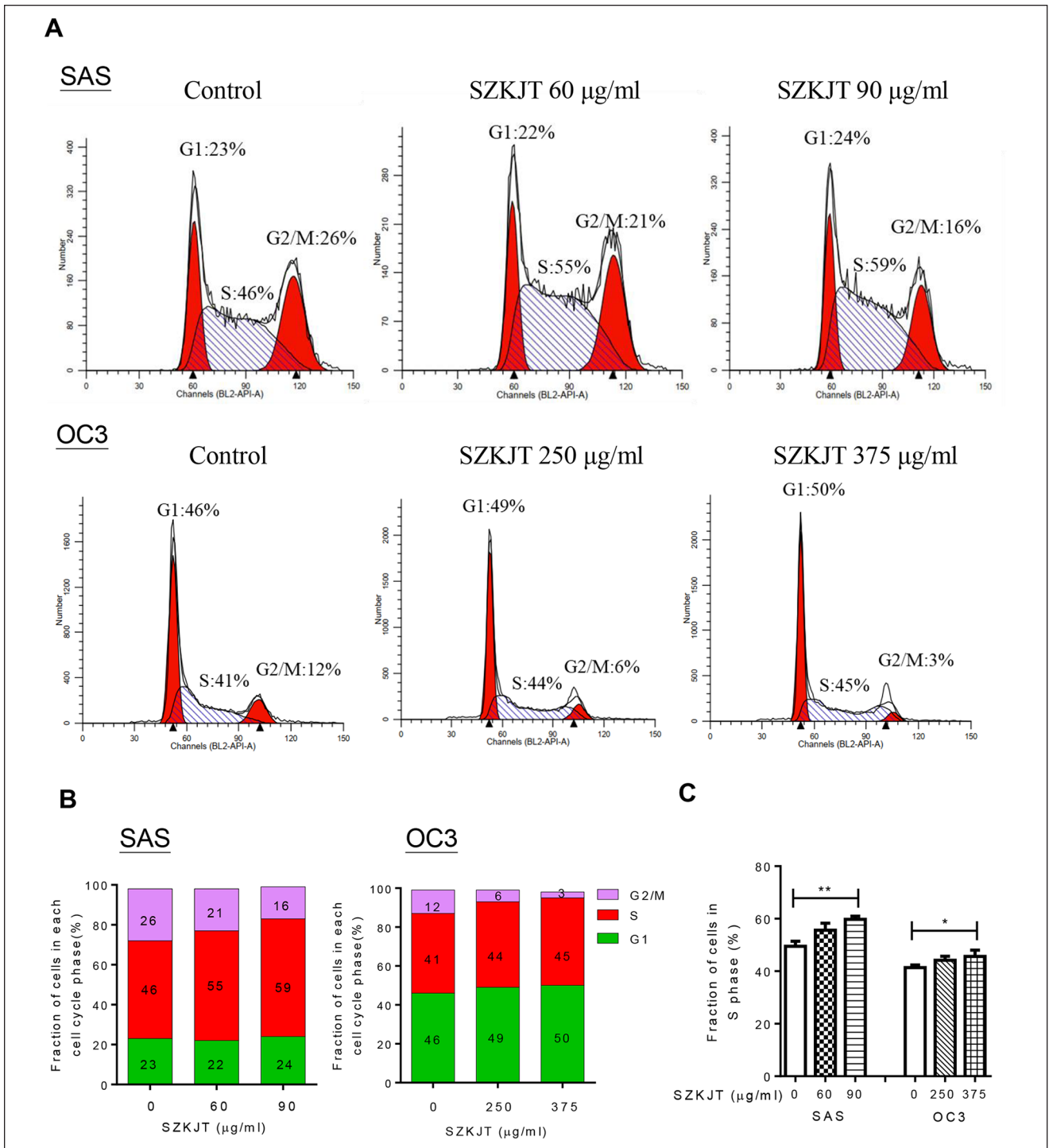


**Figure 3.** Analysis of the cell cycle distribution after SZKJT treatment. (A) Representative cell cycle distributions of SAS (upper panel) and OC3 (lower panel) cells treated with SZKJT at different doses. (B) The average percentages of SAS (left panel) and OC3 (right panel) cells in G1, S, and G2/M phases of the cell cycle are shown. (C) Fraction of cells at different phases. The results were obtained from 3 independent experiments. **\*\*** $P < .01$ ; **\*** $P < .05$ .

SZKJT treatment. In the wound healing assay, SAS and OC3 cells were pretreated with SZKJT for 24 hours in the complete medium, and the cells were then reseeded in a 6-cm plate with a 2-well insert for attachment and grown

to confluence. A defined, cell-free gap was generated by removing the insert, and the area of the cell-free gap was monitored at the indicated times (4 hours and 6 hours). As shown in Figure 5A and B, SZKJT treatment significantly

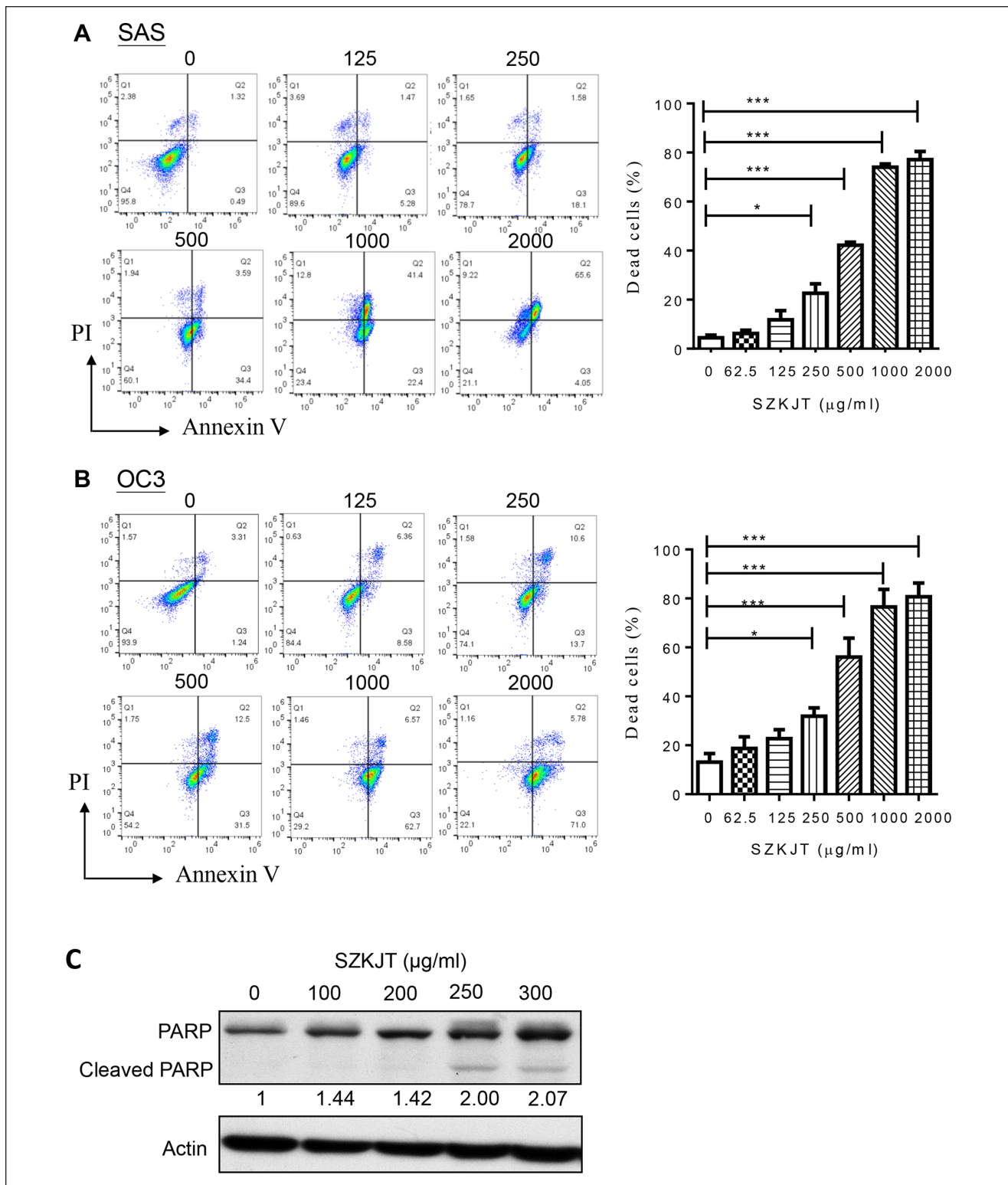


**Figure 4.** SZKJT induced OSCC cell death. Flow cytometry analysis of OSCC cells treated with a control or SZKJT at different concentrations (125, 250, 500, 1000, or 2000 µg/mL) for 48 hours. Quantification of cell death in SAS (A), and OC3 (B) cells by Annexin V-FITC/PI staining. The bar diagram shows the percentages of dead cells. The results were obtained from 3 independent experiments. \*\*\* $P < .001$ ; \* $P < .05$ . (C) Levels of the cleaved form of PARP in SZKJT-treated SAS cells were determined by western blotting.



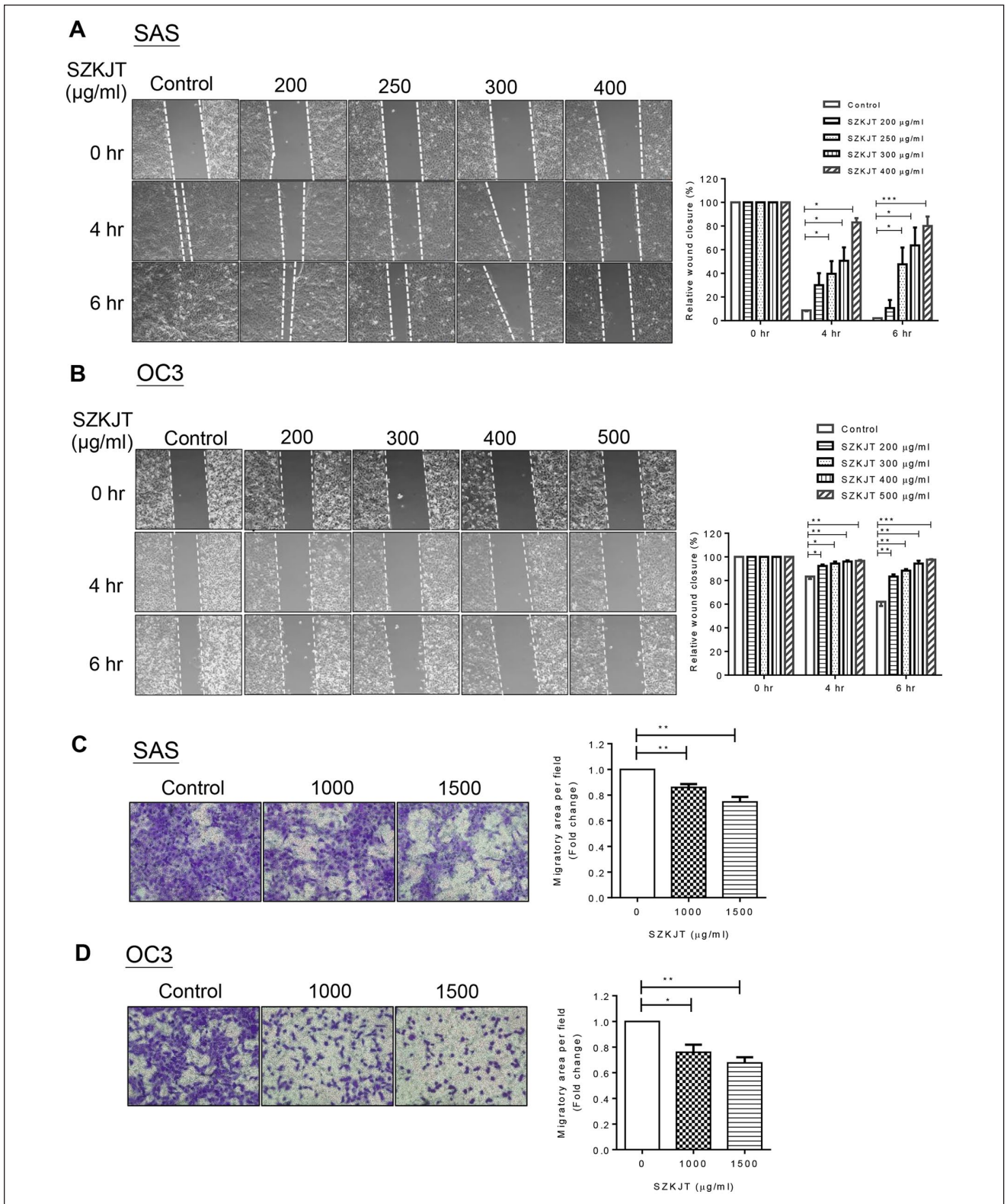


**Figure 5.** Effects of SZKJT treatment on the migration of SAS and OC3 cells. Representative images of cultured SAS (A) and OC3 (B) cells during the wound healing assay at 0, 4, and 6 hours after gap formation are shown, and the relative cell-free gap areas (%) were calculated. \*\*\* $P < .001$ ; \*\* $P < .01$ ; \* $P < .05$ . Transwell migration assay of SAS (C) and OC3 (D) cells, and their relative quantitation results. Data were represented in triplicates. \*\* $P < .01$ ; \* $P < .05$ .

inhibited the migration of SAS and OC3 tumor cells compared with migration in the control cells. Furthermore, the inhibitory effects of SZKJT on OSCC cell migration were dose- and time-dependent.

Consistent with the wound healing assay, the transwell migration assay also demonstrated that SZKJT treatment resulted in decreased migratory ability of SAS and OC3 cells (Figure 5C and D) through the porous membrane.

### ***Vimentin, Fibronectin and Oct-4 Were Downregulated, and E-cadherin was Upregulated by SZKJT***

The epithelial–mesenchymal transition (EMT) process is an important biological pathway in cancer progression in which benign tumor cells progress to malignant cells. A previous study showed a significant correlation between high vimentin-K14 expression and poor prognosis in oral cancer patients.<sup>23</sup> Additionally, together, vimentin and  $\beta 4$  integrin can be used to predict the prognosis of oral cancer.<sup>24</sup> Fibronectin was found to promote single-cell migration in highly invasive OSCC by modulating cell adhesion and signaling.<sup>25</sup> In addition, fibronectin was demonstrated to be an important biomarker and therapeutic target for the treatment of OSCC, particularly for 5-FU resistance.<sup>26</sup> The expression of vimentin and fibronectin, both of which are essential positive regulators of EMT in OSCC, was tested in SAS cells after SZKJT treatment by qPCR and western blot analysis. As shown in Figure 6A and B, the levels of vimentin and fibronectin were downregulated after the treatment of SAS cells with 250  $\mu\text{g}/\text{mL}$  SZKJT, as determined by qPCR analysis. The western blot results also showed that SZKJT attenuated the expression of vimentin and fibronectin in SAS cells (Figure 6E and F). Moreover, expression of the epithelial marker E-cadherin was increased in SZKJT-treated SAS cells (Figure 6C). Furthermore, when the expression of octamer-binding transcription factor 4 (OCT4), a marker of cancer stem-like cells (CSCs), which may contribute to cancer progression and chemoresistance,<sup>27,28</sup> was tested, the data showed that SZKJT also inhibited Oct-4 expression (Figure 6D).

### ***The Level of p-ERK was Downregulated by SZKJT***

Activation of the mitogen-activated protein kinase (MAPK) pathway, which includes p-ERK, p-JNK, and p-p38, in SAS cells was evaluated to elucidate the molecular mechanism by which SZKJT affects cell proliferation and apoptosis in OSCC. Western blot analysis showed that SZKJT inhibited the phosphorylation levels of ERK in a concentration-dependent manner (Figure 7A and B). To further demonstrate the effect of SZKJT on MEK/ERK pathway, an ERK

inhibitor PD98059 was used. The proliferation ability of SAS was inhibited when the cells were treated with PD98059 alone. Further, the combined treatment of PD98059 and SZKJT resulted in a more significant reducing proliferative activity in SAS cells (Figure 7C).

### ***SZKJT and Cisplatin Had Synergistic Anticancer Effects in OSCC***

Chemotherapy is still widely used in the early stages of OSCC or after cancer surgery. We then analyzed the potential synergistic effects of SZKJT and cisplatin in OSCC. Cells were treated with a control, 2.5  $\mu\text{M}$  cisplatin alone, or 2.5  $\mu\text{M}$  cisplatin and SZKJT at different doses for 48 hours and then assessed with an MTT assay. The results showed that cisplatin and SZKJT had a synergistic inhibitor effect on cell proliferation in SAS cells (Figure 8A), OC3 cells (Figure 8B), and OEC-M1 cells (Supplemental Figure S2). This effect was dose-dependent and more pronounced in SAS cells.

### ***SZKJT Inhibited Tumor Growth in a Xenograft Mouse Model***

We then further assessed the toxicity of SZKJT *in vivo* using immune-competent C57BL/6 mice. As shown in Figure 9A, there was no difference in body weight in the mice treated with SZKJT compared with the control group. The levels of ASL, ALT, glucose, creatinine, and albumin were comparable in the control and SZKJT-treated groups (Figure 9B and C). The complete blood counts and differential counts of white blood cells, including neutrophils, lymphocytes, monocytes, eosinophils, red blood cells, and platelets, of the control and SZKJT-treated groups were within normal ranges (Figure 9D). Finally, we tested the antitumor activity of SZKJT in tumor-bearing mice. NOD/SCID mice were SC inoculated with SAS cells for tumor growth for approximately 3 weeks, and the mice were then randomly assigned to control (300  $\mu\text{L}$  of sterile water/day, oral, 5 days per week), cisplatin (5 mg/kg, intraperitoneal injection, once per week), SZKJT (5.2 g/kg/day, oral, 5 days per week) and SZKJT (5.2 g/kg/day, oral, 5 days per week) with cisplatin (5 mg/kg, intraperitoneal injection, once per week) groups (Figure 10A). After 4 weeks of treatment, the mice were sacrificed and dissected, and the residual tumors were weighed and further processed. The volumes of the inoculated tumors were calculated twice per week. As shown in Figure 10B and C, treatment with SZKJT only or cisplatin only partially inhibited tumor growth and reduced tumor weight compared with those of the control groups. When a combination treatment with SZKJT and cisplatin was applied, the antitumor effect was more pronounced (Figure 10B and C). In addition, H&E and Ki67 staining showed that combined cisplatin and SZKJT treatment

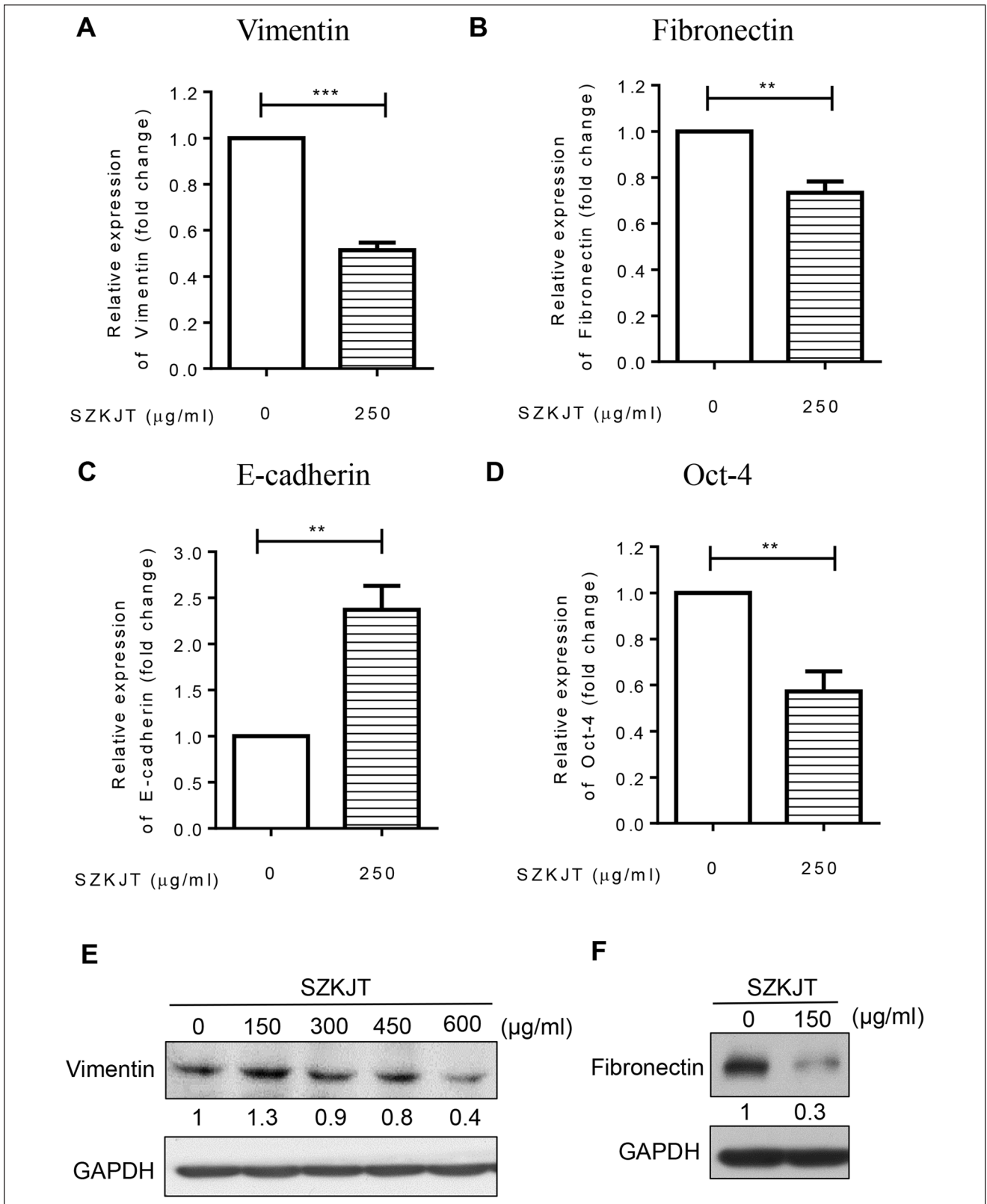


**Figure 6.** Regulatory effects of SZKJT on EMT-associated genes. The bar diagram shows the relative expression of vimentin (A), fibronectin (B), E-cadherin (C), and Oct-4 (D) after 250  $\mu\text{g/ml}$  SZKJT treatment in SAS cells, as determined by qPCR analysis. \*\*\* $P < .001$ ; \*\* $P < .01$ . Levels of the vimentin (E) and fibronectin (F) in SZKJT-treated SAS cells were determined by western blotting.

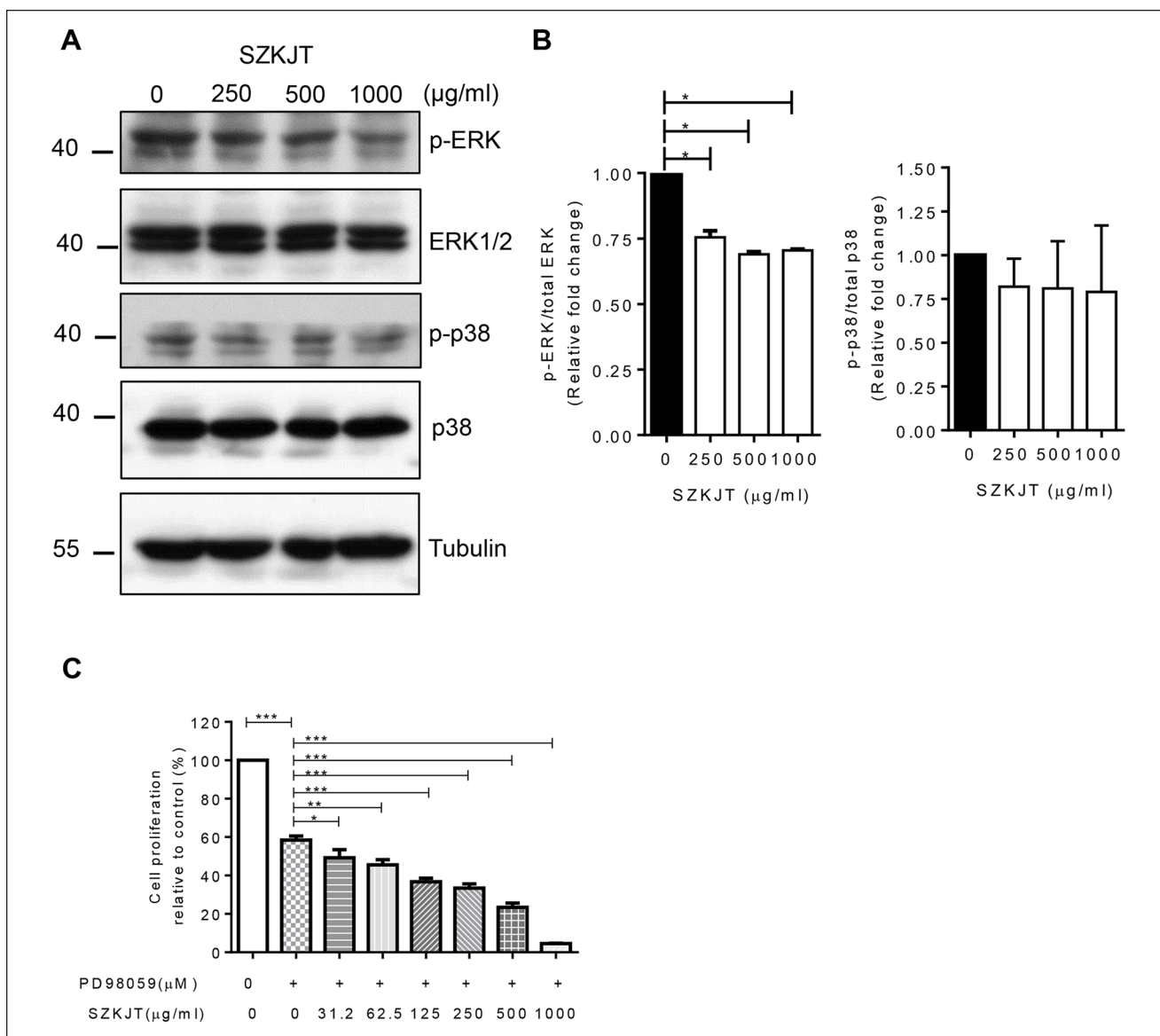


**Figure 7.** SZKJT attenuated the activation of ERK in OSCC. (A) SAS cells were treated with SZKJT (0, 250, 500, or 1000 µg/ml) for 24 hours, and the total-cell lysates were then subjected to western blotting to analyze the indicated total and phosphorylated forms of ERK and p38. (B) The bar diagram shows relative protein expression (fold change). (C) SAS cells were treated with a control, PD98059 (50 µM) alone or PD98059 (50 µM) with SZKJT at different doses (31.25, 62.5, 125, 250, 500, or 1000 µg/ml) for 48 hours and assessed by MTT assay. The results are expressed as the percent cell proliferation relative to the proliferation of the control.

inhibited tumor cell growth in the SAS cell-derived xenografts (CDXs). P-ERK levels were also reduced by combined cisplatin and SZKJT treatment, as shown by IHC staining (Figure 10D).

#### The Single Compound Baicalin or Berberine Significantly Inhibited SAS Cell Proliferation

We further tested the potential antitumor effects of the 4 major peak compounds in SZKJT (Figure 1). The single compound baicalin (Supplemental Figure S3A) or berberine

(Supplemental Figure S3B) significantly inhibited SAS cell proliferation. However, gentiopicoside and puerarin did not exert obvious antitumor effects in vitro (data not shown).

#### Discussion

Chinese herbal formulas have been used as complementary therapies for cancer in clinical practice for a long time, and their effects are more comprehensive than single herbal formulations. To better understand the effects and safety of a common Chinese herbal formula used in the clinic, the aim

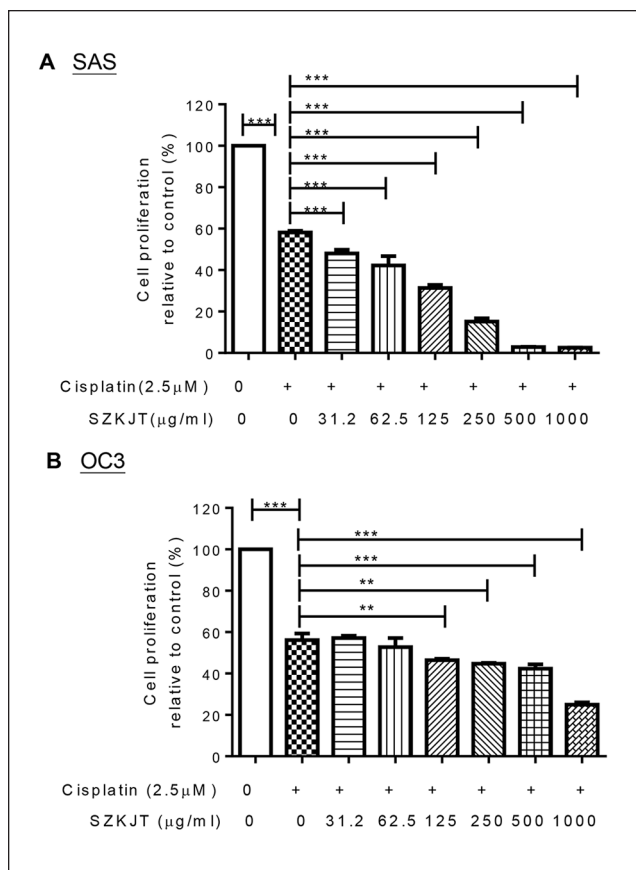


**Figure 8.** Concurrent treatment with SZKJT enhanced the therapeutic efficacy of cisplatin in OSCC cell lines. Cells were treated with a control treatment, 2.5 μM cisplatin, or 2.5 μM cisplatin with and SZKJT at different doses for 48 hours and then assessed by MTT assay. The results are expressed as the percent cell proliferation relative to the proliferation of the control. Cisplatin and SZKJT synergistically inhibited proliferation in the SAS (A) and OC3 (B) cell lines. \*\*\* $P < .001$ ; \*\* $P < .01$ .

of this study was to characterize the potential effects and molecular mechanisms of SZKJT in OSCC. Our results showed that SZKJT treatment was effective in inhibiting SAS, OC3, and OEC-M1 cell proliferation and inducing cell apoptosis. SZKJT promoted oral cancer cell cycle arrest in S phase and decreased the proportion of cells in G2/M phase. SZKJT treatment also inhibited the migration of OSCC cells. Further, we proposed the effective dual therapy of cisplatin and SZKJT that can reduce the dosage of each single drug in oral cancer. Combination treatment with cisplatin and SZKJT synergistically inhibited cell proliferation, especially in SAS cells. SZKJT at the dose of 31.25 μg/mL combined with cisplatin 2.5 μM exerted significant synergistic effects against SAS cell proliferation. Since 31.25 μg/mL of SZKJT is beneficial for combination therapy against OSCC, we used the dose range of 0 to 100 μg/mL to detect the cytotoxicity of SZKJT in

normal cells (SG cells). In SG cells, there is only 10% cell death upon 50 μg/mL SZKJT treatment by MTT assay (Supplemental Figure S4). Although greater cytotoxicity of SZKJT at higher concentrations in SG cells might be expected, the cytotoxicity of SZKJT was significantly higher in SAS cells than in normal cells. However, we did not observe toxic side effects of SZKJT on mice model as there was no difference in body weight in the mice treated with SZKJT compared with the control group. The hepatic and renal function of mice were comparable in the control and SZKJT-treated groups and the hemograms were within normal ranges in both groups. In an in vivo experiment, SZKJT also inhibited tumor growth, and a synergistic antitumor effect was demonstrated in an animal model.

The main ingredients of this formula that exert antitumor activity may be berberine and baicalin according to their antitumor potential demonstrated in our in vitro MTT assay and other previous studies.<sup>29-34</sup> Since the anticancer effects of berberine and baicalin have been studied widely in various human cancer cells, further in-depth investigation about the effects and underlying mechanisms of berberine and baicalin in treating OSCC did not conduct. In addition, the longer peak compounds within an herbal formula are not necessarily the main ingredients with antitumor effects. The active compounds within SZKJT can be further explored in the future.

Previous in vitro and in vivo studies have shown that SZKJT exhibits antitumor activity against many other types of cancer by targeting many different molecules.<sup>13-18</sup> Because the MAPK signaling pathway is important for cancer proliferation, differentiation, apoptosis, angiogenesis, invasion, and metastasis, we evaluated the effects of SZKJT on this pathway. We found that SZKJT decreased the protein levels of p-ERK but not p-JNK and p-p38 in SAS cells. Elevated ERK expression has been detected in various cancers and represents an attractive target for the development of anticancer drugs.<sup>35</sup> SZKJT was also found to increase cleaved PARP levels, as shown by western blot analysis, which could explain its ability to induce apoptosis.

Vimentin and fibronectin are important markers of cancer metastasis and can predict poor prognosis in oral cancer.<sup>23-26</sup> Vimentin and E-cadherin are tightly controlled during EMT through multiple signal transduction pathways. Upregulation of vimentin and downregulation of E-cadherin are 2 of the most critical cellular events during EMT.<sup>36</sup> Our results showed that vimentin and fibronectin were downregulated, while E-cadherin was upregulated, in SZKJT-treated SAS cells. The expression of vimentin, an intermediate filament protein, is increased in various cancers<sup>37</sup> and related to the migration and invasion of cancers. Vimentin was shown to interact with p-ERK and protect it from dephosphorylation by cell signaling.<sup>38</sup> Vimentin also promotes invasion and migration via activation of the ERK and Rac1 signaling pathways.<sup>39</sup> In OSCC, high vimentin and low E-cadherin levels are associated with an increased

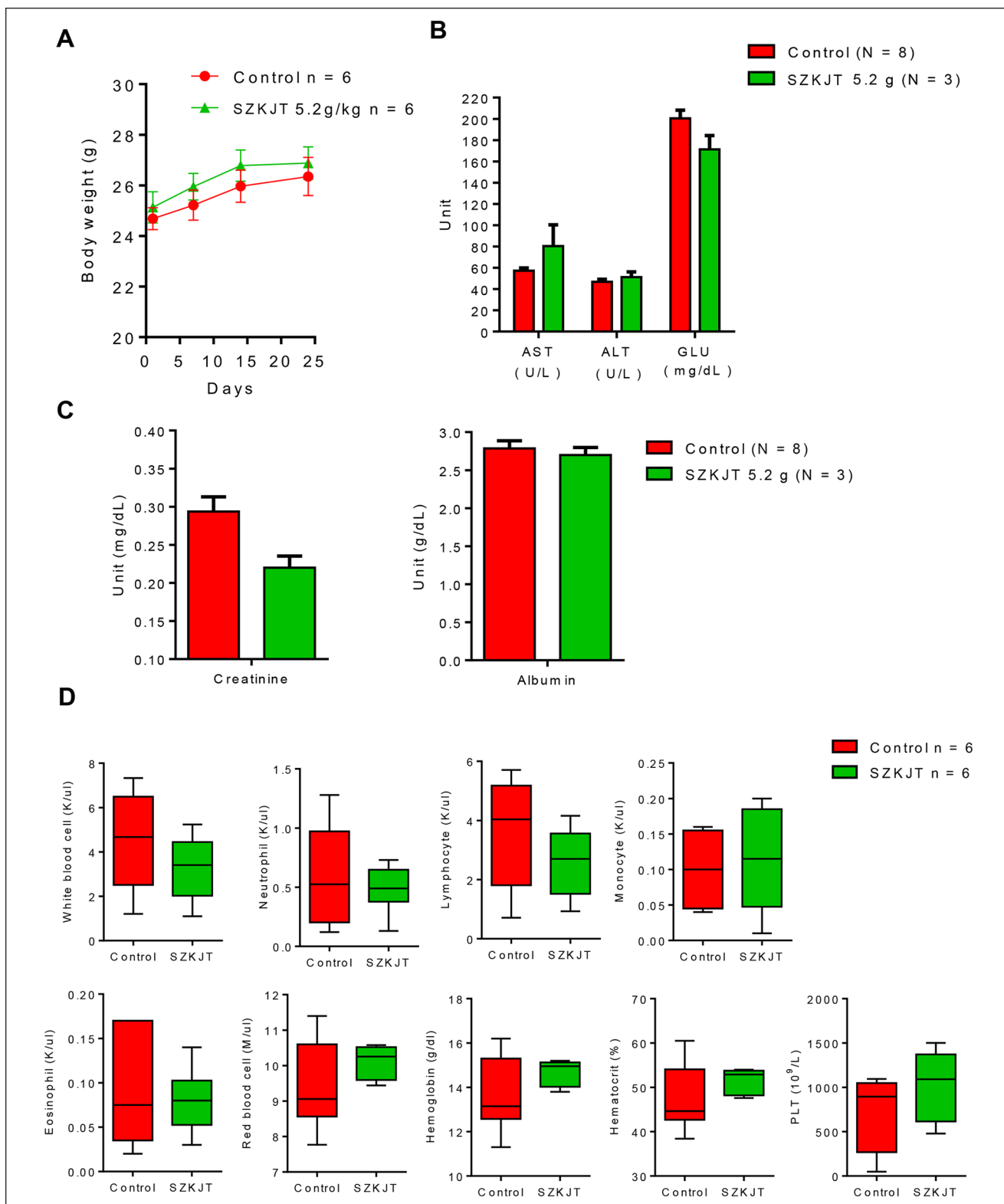


**Figure 9.** In vivo drug toxicity test. Mice were randomly assigned to the control (250  $\mu$ L of PBS, oral) group or SZKJT (5.2 g/kg, oral) group. SZKJT was given 3 times a week for 3 weeks. The body weights of the mice were recorded once per week. Blood samples were obtained from the mice before and after SZKJT treatment. (A) Curves showing the body weights of the control (250  $\mu$ L of PBS, oral, N=6) group and SZKJT (5.2 g/kg, oral, N=6) group are provided. The levels of AST, ALT, glucose (GLU) (B), creatinine, and albumin (C) and complete blood counts and differential counts (D) of the mice (N=3-8) are shown.

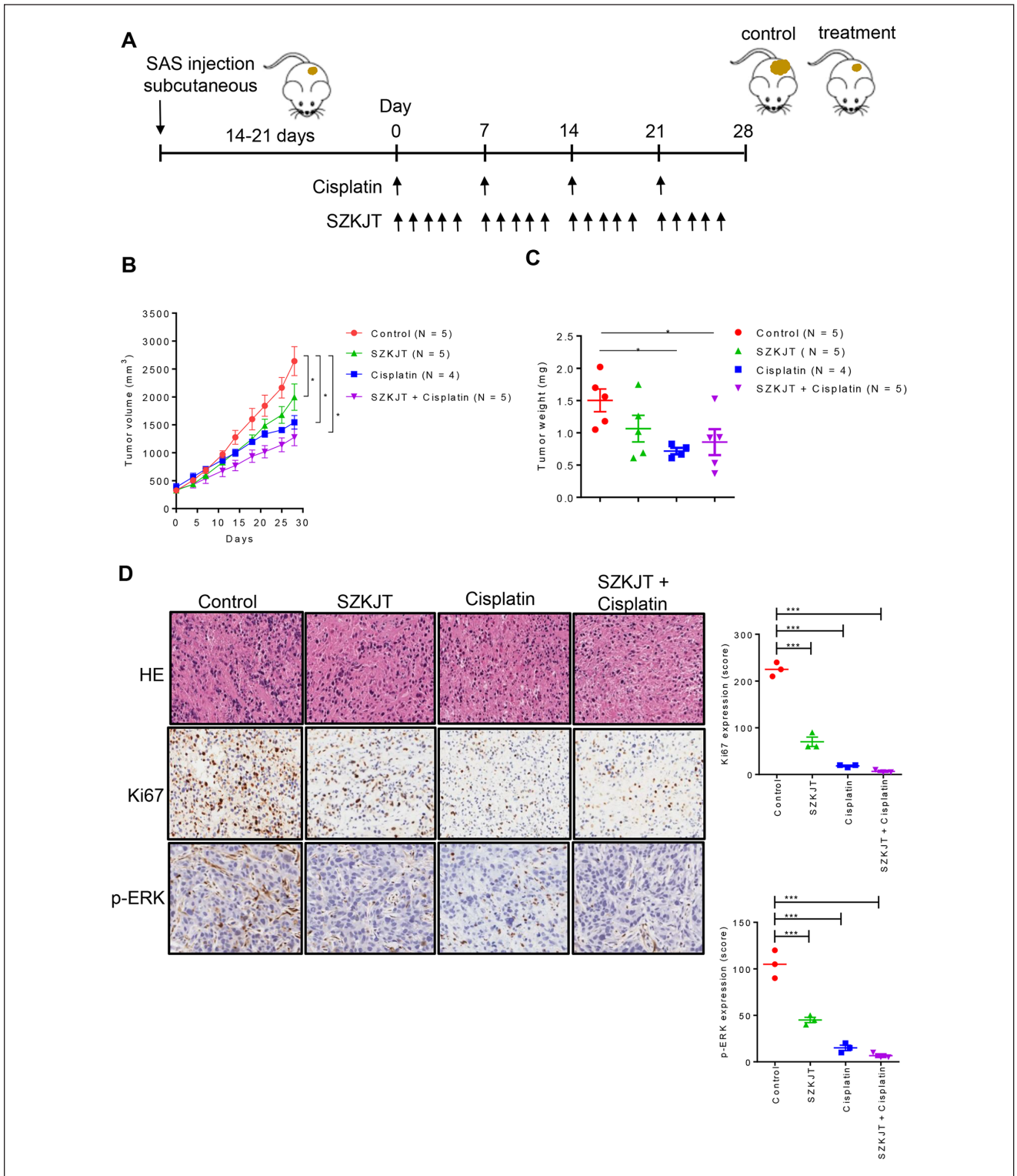


**Figure 10.** The antitumor effects of SZKJT in the xenograft mouse model. (A) The time course of the experiments. NOD/SCID mice were SC inoculated with SAS cells and then randomly assigned to the control, SZKJT (5.2 g/kg), cisplatin (5 mg/kg), and SZKJT (5.2 g/kg) plus cisplatin (5 mg/kg) groups. A detailed protocol is provided in the Materials and Methods section. (B) The volumes of the inoculated tumors before and after treatment were calculated after measurement of the tumors. (C) The tumor weights on the endpoint day are shown. (D) H&E and IHC staining for Ki67 and p-ERK in the control, SZKJT, cisplatin, and SZKJT plus cisplatin groups, with their quantitation of expression. \*\*\* $P < .001$ ; \* $P < .05$ .

rate of recurrence, distant metastasis, and poor survival.<sup>40</sup> Fibronectin, an extracellular matrix protein, is upregulated under pathological conditions, which ultimately promotes tumorigenesis, metastasis, and therapy resistance.<sup>41</sup> In addition, Oct-4, an important regulator of stemness in head and neck squamous carcinoma, and high Oct-4 expression and poor survival were found to be significantly correlated in patients with head and neck cancer.<sup>42</sup> The results herein demonstrated that SZKJT inhibited the expression of Oct-4. Furthermore, our results clearly show that the activity of SZKJT against oral cancer is mediated via ERK pathway and that SZKJT decreases EMT in OSCC.

Common side effects of cisplatin include gastrointestinal upset (which may lead to poor appetite and subsequent body weight loss), renal toxicity, and myelosuppression. The above side effects can influence patient quality of life and interfere with conventional cancer treatments. In our animal experiments, no body weight loss was observed in the mice after SZKJT treatment. All the mice showed normal renal and liver function, and blood cell counts were within normal ranges after SZKJT treatment. Since no drug toxicity was observed in the model mice, SZKJT can be used as a complementary treatment with cisplatin in the future in patients who cannot tolerate the side effects of cisplatin at a typical dose.

## Conclusion

In conclusion, this study first demonstrates the antitumor effect of SZKJT against OSCC both in vitro in tumor cell lines and in vivo in a tumor xenograft mouse model. We also explored the possible mechanisms of SZKJT against OSCC and found that it modulates the ERK pathway; downregulates vimentin, fibronectin, and Oct-4; and upregulates E-cadherin. We also provide evidence of the synergistic effects of SZKJT and cisplatin both in vitro and in vivo. Thus, this study provides evidence supporting the medical use of SZKJT for oral cancer treatment. We hope to apply these results to the clinic in the future to help reduce the side effects of conventional cancer treatments and improve the quality of life and prognosis in patients with OSCC.

## Acknowledgments

We also acknowledge the Molecular Medicine Research Center (EMRPD1M0281) and Next-Generating Sequencing Core (CLRPD1J0013), Pathology Core, and Core Instrument Center at Chang Gung University, Taoyuan, Taiwan for technical support and Chuang Song Zong Pharmaceutical Co., Ltd. for drug preparation and analysis.

## Authors Contributions

Pei-Yu Hsu and Chia-Yu Yang: conceived and designed research. Jiun-Liang Chen, Sien-Hung Yang, and Shun-Li Kuo: interpreted results of experiments. Wan-Ling Wang, Fei-Wen Jan and Chia-Yu

Yang: performed experiments. All authors read and approved the final version of this manuscript. All data were generated in-house, and no paper mill was used. All authors agree to be accountable for all aspects of work ensuring integrity and accuracy.

## Availability of Data and Materials

The data and materials are available from the corresponding author on reasonable request.

## Declaration of Conflicting Interests

The author(s) declared no potential conflicts of interest with respect to the research, authorship, and/or publication of this article.

## Funding

The author(s) disclosed receipt of the following financial support for the research, authorship, and/or publication of this article: This work was supported by grants from the Ministry of Science and Technology (MOST) to Chia-Yu Yang (MOST 110-2314-B-182-046), and Chang Gung Memorial Hospital to Pei-Yu Hsu, CMRPG5J0061 and CMRPG5J0062 and Jiun-Liang Chen, CORPG1J0021.





## Ethics Approval and Consent to Participate

The animal study protocol was approved by the Institutional Animal Care and Use Committee of Chang Gung University (IACUC Approval No. CGU107-194).

## Consent to Publish

The authors declare that they have no known competing financial interests or personal relationships that could have appeared to influence the work reported in this paper.

## ORCID iDs

Pei-Yu Hsu  <https://orcid.org/0000-0001-9719-1664>  
 Shun-Li Kuo  <https://orcid.org/0000-0002-0691-225X>  
 Sien-Hung Yang  <https://orcid.org/0000-0002-8808-3933>  
 Chia-Yu Yang  <https://orcid.org/0000-0002-5123-0856>

## Supplemental Material

Supplemental material for this article is available online.

## References

1. Siegel RL, Miller KD, Jemal A. Cancer statistics, 2018. *CA Cancer J Clin*. 2018;68:7-30.
2. Montero PH, Patel SG. Cancer of the oral cavity. *Surg Oncol Clin N Am*. 2015;24:491-508.
3. Krishna Rao SV, Mejia G, Roberts-Thomson K, Logan R. Epidemiology of oral cancer in Asia in the past decade—an update (2000-2012). *Asian Pac J Cancer Prev*. 2013;14:5567-5577.
4. Jemal A, Bray F, Center MM, Ferlay J, Ward E, Forman D. Global cancer statistics. *CA Cancer J Clin*. 2011;61:69-90.
5. Mognetti B, Di Carlo F, Berta GN. Animal models in oral cancer research. *Oral Oncol*. 2006;42:448-460.



6. Qi F, Li A, Inagaki Y, et al. Chinese herbal medicines as adjuvant treatment during chemo- or radio-therapy for cancer. *Biosci Trends*. 2010;4:297-307.
7. Dong J, Su SY, Wang MY, Zhan Z. Shenqi fuzheng, an injection concocted from Chinese medicinal herbs, combined with platinum-based chemotherapy for advanced non-small cell lung cancer: a systematic review. *J Exp Clin Cancer Res*. 2010;29:137.
8. Liu ML, Chien LY, Tai CJ, Lin KC, Tai CJ. Effectiveness of traditional Chinese medicine for liver protection and chemotherapy completion among cancer patients. *Evid Based Complement Alternat Med*. 2011;2011:291843.
9. Cho WC, Chen HY. Clinical efficacy of traditional Chinese medicine as a concomitant therapy for nasopharyngeal carcinoma: a systematic review and meta-analysis. *Cancer Investig*. 2009;27:334-344.
10. Huang YH, Chen JL, Yang SH, Liu GH, Chang KP, Tsang NM. Influence of Chinese medicine on weight loss and quality of life during radiotherapy in head and neck cancer. *Integr Cancer Ther*. 2013;12:41-49.
11. Hsu PY, Yang SH, Tsang NM, et al. Efficacy of traditional Chinese medicine in Xerostomia and quality of life during radiotherapy for head and neck cancer: a prospective pilot study. *Evid Based Complement Alternat Med*. 2016;2016:8359251.
12. Lin HC, Lin CL, Huang WY, et al. The use of adjunctive traditional Chinese medicine therapy and survival outcome in patients with head and neck cancer: a nationwide population-based cohort study. *QJM*. 2015;108:959-965.
13. Hsu YL, Yen MH, Kuo PL, et al. San-Zhong-Kui-Jian-Tang, a traditional Chinese medicine prescription, inhibits the proliferation of human breast cancer cell by blocking cell cycle progression and inducing apoptosis. *Biol Pharm Bull*. 2006;29:2388-2394.
14. Cheng CY, Lin YH, Su CC. Sann-Joong-Kuey-Jian-Tang increases the protein expression of microtubule-associated protein II light chain 3 in human colon cancer colo 205 cells. *Mol Med Rep*. 2009;2:707-711.
15. Cheng CY, Lin YH, Su CC. Sann-Joong-Kuey-Jian-Tang up-regulates the protein expression of Fas and TNF- $\alpha$  in colo 205 cells in vivo and in vitro. *Mol Med Rep*. 2010;3:63-67.
16. Chien SY, Kuo SJ, Chen DR, Su CC. Sann-joong-Kuey-jian-tang decreases the protein expression of Mcl-1 and TCTP and increases that of TNF- $\alpha$  and Bax in BxPC-3 pancreatic carcinoma cells. *Int J Mol Med*. 2013;32:85-92.
17. Su CC. Sann-Joong-Kuey-Jian-Tang decreases the protein expression of mammalian target of rapamycin but increases microtubule associated protein II light chain 3 expression to inhibit human BxPC-3 pancreatic carcinoma cells. *Mol Med Rep*. 2015;11:3160-3166.
18. Chen YL, Yan MY, Chien SY, et al. Sann-Joong-Kuey-Jian-Tang inhibits hepatocellular carcinoma Hep-G2 cell proliferation by increasing TNF- $\alpha$ , caspase-8, caspase-3 and Bax but by decreasing TCTP and Mcl-1 expression in vitro. *Mol Med Rep*. 2013;7:1487-1493.
19. Lin SC, Liu CJ, Chiu CP, Chang SM, Lu SY, Chen YJ. Establishment of OC3 oral carcinoma cell line and identification of NF-kappa B activation responses to areca nut extract. *J Oral Pathol Med*. 2004;33:79-86.
20. Yang CY, Meng CL. Regulation of PG synthase by EGF and PDGF in human oral, breast, stomach, and fibrosarcoma cancer cell lines. *Dent Res J*. 1994;73:1407-1415.
21. Decker P, Muller S. Modulating poly (ADP-ribose) polymerase activity: potential for the prevention and therapy of pathogenic situations involving DNA damage and oxidative stress. *Curr Pharm Biotechnol*. 2002;3:275-283.
22. Bressenot A, Marchal S, Bezdetnaya L, Garrier J, Guillemin F, Plénat F. Assessment of apoptosis by immunohistochemistry to active caspase-3, active caspase-7, or cleaved PARP in monolayer cells and spheroid and subcutaneous xenografts of human carcinoma. *J Histochem Cytochem*. 2009;57:289-300.
23. Dmello C, Sawant S, Alam H, et al. Vimentin regulates differentiation switch via modulation of keratin 14 levels and their expression together correlates with poor prognosis in oral cancer patients. *PLoS One*. 2017;12:e0172559.
24. Dmello C, Sawant S, Alam H, et al. Vimentin-mediated regulation of cell motility through modulation of beta4 integrin protein levels in oral tumor derived cells. *Int J Biochem Cell Biol*. 2016;70:161-172.
25. Ramos Gde O, Bernardi L, Lauxen I, Sant'Ana Filho M, Horwitz AR, Lamers ML. Fibronectin modulates cell adhesion and signaling to promote single cell migration of highly invasive oral squamous cell carcinoma. *PLoS One*. 2016;11:e0151338.
26. Nakagawa Y, Nakayama H, Nagata M, et al. Overexpression of fibronectin confers cell adhesion-mediated drug resistance (CAM-DR) against 5-FU in oral squamous cell carcinoma cells. *Int J Oncol*. 2014;44:1376-1384.
27. Villodre ES, Kipper FC, Pereira MB, Lenz G. Roles of OCT4 in tumorigenesis, cancer therapy resistance and prognosis. *Cancer Treat Rev*. 2016;51:1-9.
28. Mohiuddin IS, Wei SJ, Kang MH. Role of OCT4 in cancer stem-like cells and chemotherapy resistance. *Biochim Biophys Acta Mol Basis Dis*. 2020;1866:165432.
29. Ho YT, Yang JS, Lu CC, et al. Berberine inhibits human tongue squamous carcinoma cancer tumor growth in a murine xenograft model. *Phytomedicine*. 2009;16:887-890.
30. Ho YT, Yang JS, Li TC, et al. Berberine suppresses in vitro migration and invasion of human SCC-4 tongue squamous cancer cells through the inhibitions of FAK, IKK, NF-kappa B, u-PA and MMP-2 and-9. *Cancer Lett*. 2009;279:155-162.
31. Gong WY, Zhao ZX, Liu BJ, Lu LW, Dong JC. Exploring the chemopreventive properties and perspectives of baicalin and its aglycone baicalein in solid tumors. *Eur J Med Chem*. 2017;126:844-852.
32. Cheng CS, Chen J, Tan HY, Wang N, Chen Z, Feng Y. Scutellaria baicalensis and cancer treatment: recent progress and perspectives in biomedical and clinical studies. *Am J Chin Med*. 2018;46:25-54.
33. Zhang C, Sheng J, Li G, et al. Effects of berberine and its derivatives on cancer: a systems pharmacology review. *Front Pharmacol*. 2020;10:1461.
34. Singh S, Meena A, Luqman S. Baicalin mediated regulation of key signaling pathways in cancer. *Pharmacol Res*. 2021;164:105387.
35. Kohno M, Pouyssegur J. Targeting the ERK signaling pathway in cancer therapy. *Ann Med*. 2006;38:200-211.

36. Smith A, Teknos TN, Pan Q. Epithelial to mesenchymal transition in head and neck squamous cell carcinoma. *Oral Oncol.* 2013;49:287-292.
37. Satelli A, Li S. Vimentin in cancer and its potential as a molecular target for cancer therapy. *Cell Mol Life Sci.* 2011; 68:3033-3046.
38. Perlson E, Michaelevski I, Kowalsman N, et al. Vimentin binding to phosphorylated ERK sterically hinders enzymatic dephosphorylation of the kinase. *J Mol Biol.* 2006;364: 938-944.
39. Sharma P, Alsharif S, Fallatah A, Chung BM. Intermediate filaments as effectors of cancer development and metastasis: A focus on keratins, vimentin, and Nestin. *Cells.* 2019;8:497.
40. Nijkamp MM, Span PN, Hoogsteen IJ, van der Kogel AJ, Kaanders JH, Bussink J. Expression of E-cadherin and vimentin correlates with metastasis formation in head and neck squamous cell carcinoma patients. *Radiother Oncol.* 2011;99:344-348.
41. Wang JP, Hielscher A. Fibronectin: how its aberrant expression in tumors may improve therapeutic targeting. *J Cancer.* 2017;8:674-682.
42. Nathansen J, Lukiyanchuk V, Hein L, et al. Oct4 confers stemness and radioresistance to head and neck squamous cell carcinoma by regulating the homologous recombination factors PSMC3IP and RAD54L. *Oncogene.* 2021;40: 4214-4228.